

The nanoprodug of polytemozolomide combines with MGMT siRNA to enhance the effect of temozolomide in glioma

Haoyue Xu^a, Yongkang Zhang^a, Linfeng Li^a, Yanhong Ren^a, Feng Qian^a, Lansheng Wang^a, Hongwei Ma^a, Ankang Quan^a, Hongmei Liu^{a,c} and Rutong Yu^{a,b}

^aInstitute of Nervous System Diseases, Xuzhou Medical University, Xuzhou, China; ^bDepartment of Neurosurgery, Affiliated Hospital of Xuzhou Medical University, Xuzhou, China; ^cDepartment of Biomedical Engineering, Southern University of Science and Technology, Shenzhen, China

ABSTRACT

Temozolomide (TMZ) is a conventional chemotherapeutic drug for glioma, however, its clinical application and efficacy is severely restricted by its drug resistance properties. O6-methylguanine-DNA methyltransferase (MGMT) is a DNA repair enzyme, which can repair the DNA damage caused by TMZ. A large number of clinical data show that reducing the expression of MGMT can enhance the chemotherapeutic efficacy of TMZ. Therefore, in order to improve the resistance of glioma to TMZ, an angioprep-2 (A2) modified nanoprodug of polytemozolomide (P(TMZ)n) that combines with MGMT siRNA (siMGMT) targeting MGMT was developed (A2/T/D/siMGMT). It not only increased the amount of TMZ within tumor lesion site, but also reduced MGMT expression in glioma. The *in vitro* experiments indicated that the A2/T/D/siMGMT effectively enhanced the cellular uptake of TMZ and siMGMT, and resulted in a significant cell apoptosis and cytotoxicity in the glioma cells. The *in vivo* experiments showed that glioma growth was inhibited and the survival time of animals were prolonged remarkably after A2/T/D/siMGMT was injected via tail vein. The results showed that the therapeutic effect of A2/T/D/siMGMT in the treatment of glioma was significantly improved.

ARTICLE HISTORY

Received 29 September 2022
Revised 18 November 2022
Accepted 21 November 2022

KEYWORDS

Glioma; drug-resistance; siMGMT; P(TMZ)n

Introduction

Glioma can emerge in different parts of the central nervous system (CNS), which is known as the most common and deadliest primary malignant brain tumor (Yang et al., 2022; Tan et al., 2020). The standard treatment of glioma is customized to the individual patient, including chemotherapy, radiation therapy, surgery or observation (Otvos et al., 2021). However, because of the ability to invade/infiltrate and genetic heterogeneity, the therapeutic effect of glioma remains unsatisfactory (Nicholson & Fine, 2021; Johnson et al., 2021). Moreover, the ability to deliver the chemotherapeutic drug to the tumor site is limited by the blood-brain barrier (BBB), a highly specialized structure of the vascular tree that restricts diffusion and transport from the blood to the brain (Islam et al., 2021; Hanafy et al., 2021). This also contributes to the poor survival and prognosis of glioma. The five-year survival rate is only 5.6%, with a median overall survival duration of 14.6 months (Wang et al., 2021; Karlsson et al., 2021). As a result, post-operative chemotherapy in combination with surgery is critical for individuals with brain gliomas.

TMZ, an alkylating agent, is the first-line drug that has been applied for the treatment of malignant glioma for over a decade (Tan et al., 2020; Qiao et al., 2018; Zhang et al., 2021). It spontaneously converts into its metabolite

5-(3-methyltriazene-1-yl) imidazole-4-carboxamide (MTIC), which alkylates DNA and induces cell death *in vivo*. Malignant glioma resistance to TMZ has become a significant clinical issue (Meng et al., 2020). Glioma cells gain TMZ-resistance through a complex mechanism, in which MGMT is one of the most critical contributors. Relating literatures illustrate that MGMT can repair DNA alkylation damage caused by alkylating agents, which is the main reason for glioma cells to develop drug resistance to TMZ (Wang et al., 2021). Therefore, it is more meaningful to conquer the problem of TMZ-resistance than to develop a new target drug in the treatment of malignant brain glioma. A large number of studies show that reducing the expression of MGMT can enhance the efficacy of TMZ (Wang et al., 2021). Moreover, the effectiveness of TMZ in clinical treatment is limited because of the following problems: 1) short half-life (Du et al., 2020); 2) difficulty of penetrating the BBB (Tian et al., 2021); 3) toxic to normal tissues (Jiang et al., 2021). Therefore, overcoming resistance of glioma to the chemotherapeutic TMZ is a key method in treatment strategies.

RNA interference (RNAi), a high efficiency and low toxicity strategy, has been very successfully applied as a gene-silencing technology (Xu et al., 2022). The United States (US) Food and Drug Administration (FDA) has approved the application of

CONTACT Yu Rutong  rtyu@xzhmu.edu.cn; Hongmei Liu  liuhongmei816@sina.com  Institute of Nervous System Diseases, Xuzhou Medical University, Xuzhou, China

 Supplemental data for this article can be accessed online at <https://doi.org/10.1080/10717544.2022.2152911>.

*These authors contributed equally to this work.

© 2022 The Author(s). Published by Informa UK Limited, trading as Taylor & Francis Group.

This is an Open Access article distributed under the terms of the Creative Commons Attribution-NonCommercial License (<http://creativecommons.org/licenses/by-nc/4.0/>), which permits unrestricted non-commercial use, distribution, and reproduction in any medium, provided the original work is properly cited.

siRNA therapy for clinical practice (Setten et al., 2019; Zoulikha et al., 2022; Joshi et al., 2020). Based on the biological safety and clinical application prospect of siRNA, it is more valuable to use siRNA to silence the expression of MGMT (Liu et al., 2019; Sita et al., 2017).

Herein, we synthesized P(TMZ)n by chemical method and constructed a drug delivery system for co-delivering P(TMZ)n and siMGMT into glioma cells, in the hope of reducing the expression of MGMT and enhancing the sensitivity of TMZ in glioma. In this study, we developed a responsive (matrix metalloproteases, MMPs) nanoparticle (A2/T/L/siMGMT) by self-assembling a small-molecule amphiphile, triglycerol monostearate (Joshi et al., 2018) (TG-18) to achieve local P(TMZ)n and siRNA delivery. A2/T/D/siMGMT could promote the penetration of siMGMT across the BBB and protect siMGMT from degradation. Meanwhile, the degradable ester bond of P(TMZ)n was hydrolyzed and TMZ was released in the low pH environment of glioma (Hua et al., 2018). In addition, the combined delivery of P(TMZ)n and siMGMT decrease the expression of MGMT and enhance the sensitivity of TMZ on glioma cells, consequently increasing its anti-tumor activity both in vitro and in vivo.

Materials and methods

Materials

DSPE-PEG-2000 was obtained from Meilun Biotechnology Co., Ltd (Dalian, China). P(TMZ)n was synthesized from Beixin Biotechnology Co., Ltd (Suzhou, China). 4',6-diamidino-2-phenylindole dihydrochloride (DAPI) and 1,2-dioleoyl-3-trimethylammoniumpropane (DOTAP) were purchased from Sigma-Aldrich (Saint Louis, MO, USA). AnnexinV-fluorescein isothiocyanate (FITC)/propidium iodide (PI) was obtained from Nanjing Key GEN BioTECH Co. Ltd (Nanjing, China). Calcein/PI Live/Dead Viability/Cytotoxicity Assay Kit were purchased from Beyotime Biotechnology. Angiopep-2 (TFFYGGSRGKRNNF KTEEY) was purchased from GLBiochem Ltd (Shanghai, China). Cell Counting Kit-8 (CCK8) and D-Luciferin potassium were purchased from Meilun Biotechnology Co., Ltd (Dalian, China). LysoTracker™ green was brought from Invitrogen (Carlsbad, CA, USA). MGMT Rabbit monoclonal antibody (mAb) was got from Cell Signaling Technology Co., Ltd (Danvers, MA, USA). Beta-actin mAb was bought from Protein tech Antibodies People Trust (Chicago, IL, USA). Cy5-labeled siRNA (Cy5-siRNA), negative control siRNA with a scrambled sequence (nonsense, antisense strand, 5'-UCGAAGUACUCAGCGUAAGdTdT-3'), and siRNA targeting MGMT mRNA (siMGMT, antisense strand, 5'-UGUCGCUCAAACAUCdTdT-3') were purchased from Beixin Biotechnology Co., Ltd (Suzhou, China).

Methods

Synthesis of P(TMZ)n

TMZ is dissolved in concentrated sulfuric acid, and the solution is cooled to 0°C under the protection of nitrogen. Sodium nitrite aqueous solution was dropped into the above

sulfuric acid solution, and stirred to room temperature in the dark. The reaction solution was cooled to 0°C, stirred and precipitated to produce TMZ-carboxylic acid. TMZ-carboxylic acid and hydroxyethyl methacrylate were dissolved in dichloromethane respectively, and DMAP and EDC were added to the TMZ-carboxylic acid solution in dichloromethane, and reacted under nitrogen protection to form TMZ-metacrylate.

P(TMZ)n was synthesized by living free radical polymerization

According to the different polymerization degree (DP), TMZ methylate, ethyl 2-iodo-2-phenylacetate and V-501 were co dissolved in anhydrous dimethylformamide DMF at a certain molar ratio and reacted at 70°C for 24 hours. After that, it was purified with ice ether under the protection of nitrogen.

Nanoparticle preparation and characterization

Angiopep-2 (0.12 mg) and DSPE-PEG2000 (1 mg) were added to DMSO (1 mL) and the mixture was stirred vigorously for 24 h. The released 2-pyridinethione was measured to characterize the obtained product. Then, the reaction mixture was dialyzed against deionized water in a dialysis bag (MWCO 3500 Da), and lyophilized to acquire A2-DSPE-PEG2000.

DOTAP and P(TMZ)n were dissolved in DMSO, siRNA was dissolved in nuclease-free water, and then a predefined amount of siMGMT aqueous solution was mixed with DOTAP lipid molecule in DMSO solution to obtain D/MsiRNA. The mixed solution of D/MsiRNA and P(TMZ)n (2 mg), TG18 (0.4 mg), and A2-DSPE-PEG2000 (0.12 mg) was slowly dropped into water, stirred vigorously for 1 h, and the DMSO was removed by dialysis to obtain A2/T/D/siMGMT. Meanwhile, A2/T/D/CsiRNA was prepared by the same method, in which siMGMT was replaced with control siRNA (CsiRNA).

The size, zeta potential and stability in serum of nanoparticles were detected by Malvern Mastersizer. The morphology of Nanoparticle was observed by Transmission Electron Microscope (TEM, Tecnai G2 Spirit Twin).

Gel retardation assay

Agarose gel electrophoresis was used to estimate the binding capacity of siRNA to DOTAP. 2% (w/v) agarose gel containing ethidium bromide (EtBr 0.5 µg·mL⁻¹) was used for agarose gel electrophoresis. Complexes of siRNA were prepared for electrophoresis at various N/P ratios (0, 0.3, 0.5, 1 and 1.5). Samples were performed for 15 minutes at 110V. Results were visualized by UV exposure.

In vitro release studies of A2/T/D/siMGMT

The solution of A2/T/D/Cy5-siMGMT was transferred to a dialysis membrane (MWCO 15 kDa), and immersed it in PBS (50 ml) with MMP9 (1 µg·mL⁻¹). At different times, removed 1 mL of PBS solution in the tube and centrifuged for about 20 minutes. Then, the supernatant was collected and detected Cy5 with a microplate reader (650 nm). Finally, refilled the tube again with 1 mL of PBS (Basuki et al., 2013).

Cell culture

Glioma cell lines were received from the Shanghai Cell Bank, Chinese Academy of Sciences. All Cells were cultured in DMEM containing 10% heat-inactivated Fetal Bovine Serum (FBS) and 1% Penicillin Streptomycin Solution. Cells were maintained in a humidified incubator at 37°C in 5% CO₂ and 95% air (Kang et al., 2020).

The construction of U87^{MGMT} cell line

The U87 cell line were purchased from the Shanghai Cell Bank, Chinese Academy of Sciences. Cells were cultured in DMEM contained with 10% fetal bovine serum and 1% penicillin, streptomycin and incubated at 37°C with a humidified atmosphere of 5% CO₂. The pCDH-CMV-Luci-MGMT and pCDH-CMV-MCS-3×FLAG-EF1a-CopGFP-T2A-Puro-WPRE lentiviruses were purchased from Genechem. After transfection by the lentiviruses for 48 hours, the cells were cultured with 4 µg·ml⁻¹ puromycin. The surviving cells were used in the subsequent experiments. The overexpression MGMT of U87^{MGMT} cell line was checked by Westernblot and qRT-PCR.

Cellular uptake

Cy5-siRNA was used as a fluorescent probe for NPs to assess their cellular uptake. T98G cells were inoculated in 12-well dishes at a density of 5×10⁴ cells/1 mL/well and incubated 24 hours at 37°C in a humidified air with 5% CO₂. free Cy5-siRNA, T/D/Cy5-siRNA and A2/T/D/Cy5-siRNA were added at a dose of siRNA 1 µg·mL⁻¹ (including 20% Cy5-siRNA). After 4 hours, the cells were washed 3 times with PBS. Then, the cells were fixed in 4% paraformaldehyde and stained by 4',6-diamidino-2-phenylindole (DAPI) measured by laser confocal microscopy (Olympus, Tokyo Japan). T98G cells were inoculated in 6-well dishes at a density of 1×10⁵ cells/2 mL/well and incubated 24 hours at 37°C in a humidified air with 5% CO₂. free Cy5-siRNA, T/D/Cy5-siRNA and A2/T/D/Cy5-siRNA were added at a dose of Cy5-siRNA 1 µg·mL⁻¹. The cells were washed for 3 times with PBS. After that, the cells were harvested for flow cytometry. T98G cells were inoculated in 6-well dishes at a density of 1×10⁵ cells/2 mL/well and incubated 24 hours at 37°C in a humidified air with 5% CO₂. free Cy5-siRNA, T/D/Cy5-siRNA and A2/T/D/Cy5-siRNA were added at a dose of Cy5-siRNA 1 µg·mL⁻¹. The cells were washed for 3 times with PBS. After that, the cells were harvested for flow cytometry.

In vitro cytotoxicity assay

The cytotoxicity of the nanocomplexes was assessed using the Cell Counting Kit-8 (CCK8). T98G, U87 and U87^{MGMT} cells were incubated in 96-well plates at a density of 5×10³ cells/well. PBS, free TMZ, A2/T/D/CsiRNA and A2/T/D/siMGMT were added respectively after 24 hours and the concentration of siRNA was 1 µg·mL⁻¹. Cells were cultured for 48 h, then CCK8 solution was added to each well and incubated for an additional 1 h. Optical density (OD) at 450 nm was determined using spectrophotometric analysis.

Cell apoptosis study

T98G and U87^{MGMT} cells were seeded in 6-well plates at a density of 1×10⁵ cells/well and incubated at 37°C in 5% CO₂ for 24 hours. Cells were treated with different formulations (PBS, free TMZ, A2/T/D/CsiRNA, A2/T/D/siMGMT). The dose was 100 µM TMZ and 1 µg·mL⁻¹ siRNA. After 24 h, cells were collected, washed three times with PBS and resuspended in 500 µL of buffer. Then, 5 µL of Annexin V-FITC and 5 µL of PI were added and incubated with the cells for 15 minutes in the dark. Finally, apoptosis was detected by flow cytometry.

Quantitative real-time reverse transcription polymerase chain reaction analysis (qRT-PCR)

First, primers are designed according to the mRNA of the cell-specific gene (Primer Sequence [5'-3'] F: the primers (5'-3') GCGCAAGCTTCCATGCTGGGACAGCCCCGC and R: GCGCGAATTCGTTTCGGCCAGCAGGCGGG). Then, RNA was extracted using TRIzol[®] Reagent (Tiangen, Beijing, China) according to the manufacturer's instructions. Next, cDNA was synthesized refer to the kit (Reverse Transcription, RT). Finally, mRNA was quantified using qPCR in an ABI 750 machine (ABI, Foster City, CA, USA). GAPDH mRNA levels were used as the internal reference standard.

Live/dead assay

Cells were seeded in 12-well dishes and incubated for 24 hours. Subsequently, cells were washed twice with PBS before adding the fluorochrome according to the instructions (Keygen Bio) and incubated for another 45 min. Fluorescence images were tested by OLYMPUS TH4-200 fluorescence microscopy.

EdU cell proliferation assay

To assess cell proliferation, glioma cells were seeded in 96-well culture plates at a density of 5×10³. After 24 hours of incubation (37°C and 5% CO₂), PBS, free TMZ, A2/T/D/CsiRNA and A2/T/D/siMGMT were added into different groups, respectively. In 48 hours, cells were incubated with 50 mM EdU for 2 h, followed by fixation, permeabilization, and DAPI staining according to the manufacturer's instructions. Finally, the proportion of EdU positive cells was determined by fluorescence microscopy (Olympus, Tokyo Japan).

Western blotting analysis

T98G and U87^{MGMT} cells (2×10⁵) were seeded in 6-well culture plates and incubated at constant temperature for 24 hours. PBS, free TMZ, A2/T/D/CsiRNA and A2/T/D/siMGMT were added into different groups at a dose of siRNA 1 µg·mL⁻¹. After 48 hours, cells were harvested and proteins were extracted. The quantity and balance of extracted protein samples were tested by BCA kit (Beyotime, Shanghai, China). Proteins were then separated using SDS-PAGE and transferred to nitrocellulose membranes using a semi-dry blotter (Invitrogen). Then, the membranes were incubated with primary antibodies (E9O4V) (86039, 1:1000) and exposed to

X-ray films. Finally, band gray values were quantified by Image J.

Glioma model

Male BALB/c nude mice (5-8 weeks) were purchased from Beijing Life River Laboratory Animal Technology Co., Ltd. with the approval of the Animal Care and Use Committee of Xuzhou Medical University, China (NO.202106A120). 5×10^5 U87^{MGMT-Luci} cells were suspended in 5 μ L of L15 medium and injected into the right striatum of mice to establish a glioma model. A week later, the D-Luciferin potassium (15 mg·mL⁻¹) was injected intravenously into each mouse (10 mg·kg⁻¹) and luciferin was measured using an in vivo imaging system (Caliper, Princeton, NJ, USA). Luciferase fluorescence intensity to determine the successful construction of a glioma model. Subsequently, nude mice were divided into 4 groups ($n=7$) according to fluorescence intensity.

Biodistribution studies

The glioma model was successfully constructed. PBS, free Cy5-siRNA and A2/T/D/Cy5-siRNA (the dose of Cy5-siRNA was 1 mg·kg⁻¹) then were injected into mice through the tail vein, respectively. After 4 h, the nude mice were sacrificed. Brain and its organs (heart, liver, spleen, lung, and kidney) were collected for fluorescence imaging. The Cy5 (650 nm, 670 nm) fluorescence intensity was observed with an in vivo imaging system (Caliper, Princeton, NJ, USA).

In vivo antitumor efficacy

After 7 days of U87^{MGMT} cells were implanted, mice were divided into 4 groups ($n=7$). PBS, free TMZ, A2/T/D/CsiRNA and A2/T/D/siMGMT were injected into different groups via tail vein, respectively. All groups received treatment with TMZ (10 mg·kg⁻¹) and siRNA (1 mg·kg⁻¹) on days 9, 11, 13 and 15. On days 17 and 27, mice were imaged again using the intravital imaging system. Meanwhile, T1-weighted (T1W) MRI was observed using a 7T magnetic resonance imaging (MRI) instrument (PharmaScan, Bruker BioSpin MRI GmbH, Germany) (Xu et al., 2020). The survival time of the mice in each group was observed, and the body weight of the mice was recorded every two days.

Blood pharmacokinetics

Free Cy5-siRNA and A2/T/D/Cy5-siRNA (Cy5-siRNA dose of 1 mg·kg⁻¹) were injected into mice and used to determine pharmacokinetics. Then, 40 μ L of venous blood samples were collected from caudal vein at different time points (5 min, 10 min, 0.5 h, 1 h, 2 h, 4 h, 8 h, 12 h, 24 h). The Cy5 concentration was assayed by the fluorescence microplate reader (650 nm, 670 nm).

Histology staining and organ safety evaluation

On days 9, 11, 13 and 15, different groups of U87^{MGMT-Luci} tumor-bearing mice were injected with PBS, free TMZ, A2/T/D/CsiRNA and A2/T/D/siMGMT, according to the doses of TMZ (10 mg·kg⁻¹) and siRNA (1 mg·kg⁻¹), respectively. After the last

treatment, three mice in each group were sacrificed, and their organs (heart, liver, spleen, lung, and kidney) and blood samples were collected for histological examination and biochemical laboratory of blood. Brain tissues were prepared from pathological sections for TUNEL and Ki-67 immunostaining analysis.

Statistical analysis

Data were statistically analyzed using analysis of one-way ANOVA and Student's t-test. Results were represented as mean and mean \pm SD in the graph (* $P < 0.05$, ** $P < 0.01$, *** $P < 0.001$).

Results

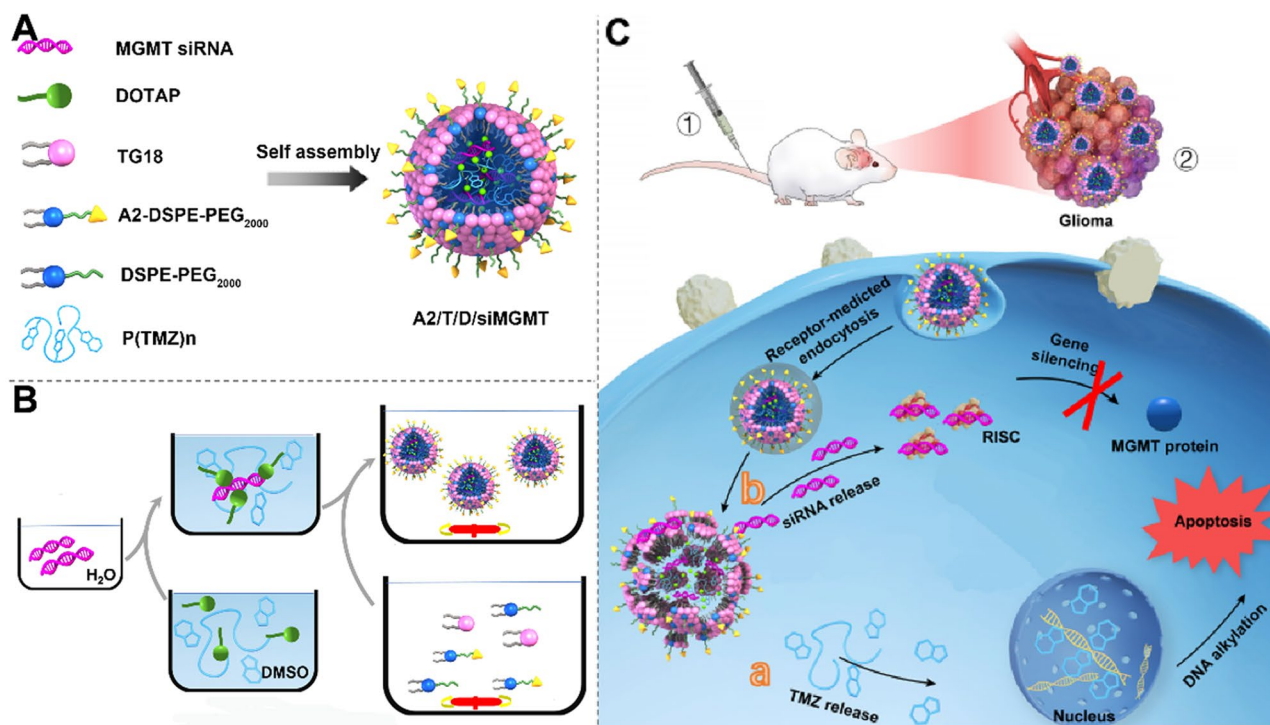
Preparation and characterization of A2/T/D/siMGMT

In the Figure S1, P(TMZ)_n with polymerization degree of 14, 29, 35 were synthesized according to the steps in Figure S2. GPC results showed a narrow molecular weight distribution of P(TMZ)₂₉ with PDI of 1.3 (Table S1). ¹H NMR spectroscopy fully confirmed the chemical structure of P(TMZ)₂₉ in Figure S3. The naked siMGMT was easily complexed with the cationic lipid materials (DOTAP) by the electrostatic interaction and P(TMZ)₂₉ was hydrophobic core to form the A2/T/D/siMGMT (Scheme 1).

As shown in Figure 1(A), the average particle size of A2/T/D/siMGMT was 61.71 ± 1.5 nm (Figure 1A [a]). The hydrodynamic diameters showed that the A2/T/D/siMGMT were degraded in MMP9 environment (Figure 1A [b]). The same results as the hydrodynamic diameter were obtained by the TEM image (Figure 1(D)). Besides, the zeta potential of A2/T/D/siMGMT was 3.743 ± 5.064 (Figure 1B [a]). The potential of A2/T/D/siMGMT in MMP-9 environment was heterogeneous (Figure 1B [b]). These results suggested that nanoparticles can be cleaved responsively in the glioma microenvironment.

Agarose gel electrophoresis experiment showed that siMGMT was completely adsorbed by DOTAP when the N/P ratio was 1.5: 1 (Figure 1(C)). Hence we choose this ratio for subsequent experiments. When the particle size change of A2/T/D/siMGMT in serum was measured at room temperature, the size remained constant during 5 days (Figure S4). This indicated that NPs have good stability in plasma. Besides, the characterization of A2/T/D/CsiRNA was exhibited in Figure S5.

As previously reported, the invasiveness and infiltration of glioma cells is achieved by increasing matrix metalloproteinases (MMPs). Thus, the expression of MMPs is upregulated in the glioma microenvironment (Kleber et al., 2008). The ability of the A2/T/D/Cy5-siMGMT to release the encapsulated drug in the presence of MMPs was evaluated. Therefore, nanoparticles were incubated in PBS (pH 7.4) at 37 °C without or with MMP-9 (1 μ g·mL⁻¹). A2/T/D/Cy5-siMGMT demonstrated excellent stability to nonspecific hydrolysis in PBS, and MMP-9 resulted in significantly higher cumulative drug, with more than 60% cumulative release of Cy5 and TMZ over a period of 72 hours (Figure S6).



Scheme 1. Schematic illustration of the A2/T/D/siMGMT drug formation and delivery system. (A) (B) The formation and the main components of A2/T/D/siMGMT. (C) After intravenous (i.v.) injection, the A2/T/D/siMGMT preferentially accumulate in glioma by receptor mediated transcytosis (RMT) strategy and internalize through endocytosis, then A2/T/D/siMGMT escape from the endosomal and release the TMZ and siMGMT, the siMGMT silence the MGMT gene, thereby enhance the efficacy of TMZ in treating glioma.

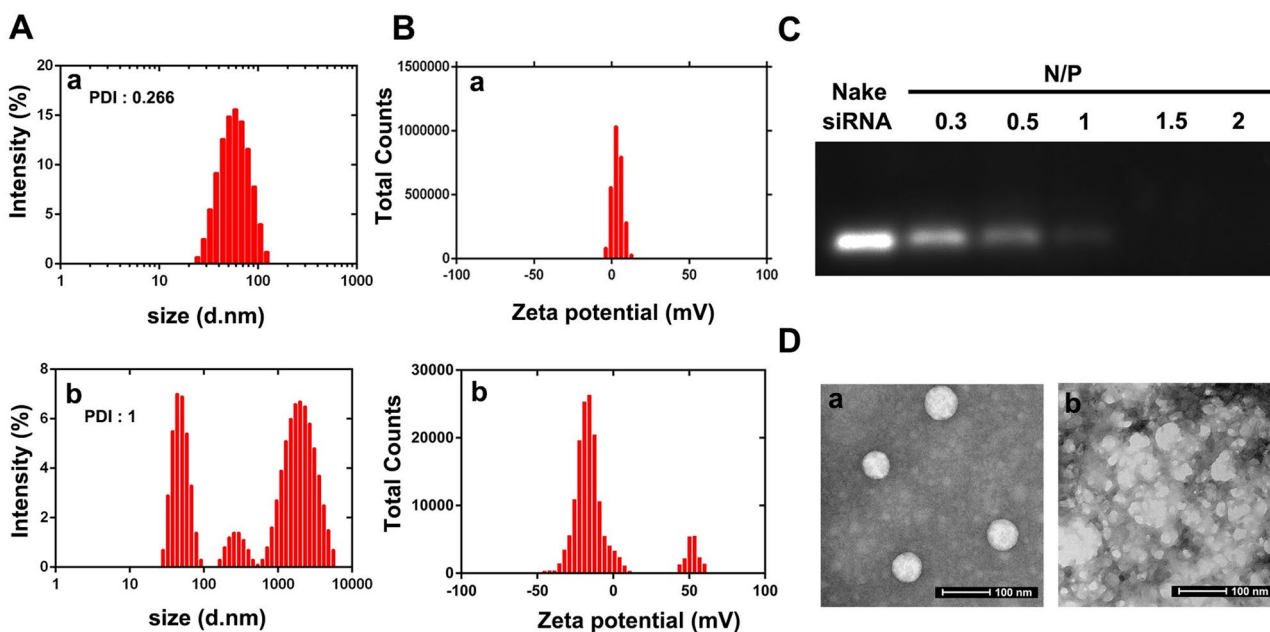


Figure 1. Preparation and characterization of A2/T/D/siMGMT. (A) The particle size distribution of A2/T/D/siMGMT in PBS without (a) or with (b) MMP-9 ($1 \mu\text{g}\cdot\text{ml}^{-1}$). (B) The zeta potential of A2/T/D/siMGMT in PBS without (a) or with (b) MMP-9 ($1 \mu\text{g}\cdot\text{ml}^{-1}$). (C) Gel retardation assay of binding capacity of siMGMT at various N/P ratios. (D) TEM image of A2/T/D/siMGMT in PBS without (a) or with (b) MMP-9 ($1 \mu\text{g}\cdot\text{ml}^{-1}$).

Cellular uptake and endosomal escape

After T98G cells were incubated with free Cy5-siRNA, T/D/Cy5-siRNA and A2/T/D/Cy5-siRNA, the drug uptake was investigated by fluorescence microscope and flow cytometry, respectively. As shown in Figure 2(A) and (B), the results of

cellular uptake experiment indicated that cells treated with A2/T/D/Cy5-siRNA exhibited the strongest Cy5-siRNA fluorescence, which was significantly different from other groups (Figure 2(C)). The result indicated that the modification of A2 enhanced the cellular uptake of A2/T/D/Cy5-siRNA.

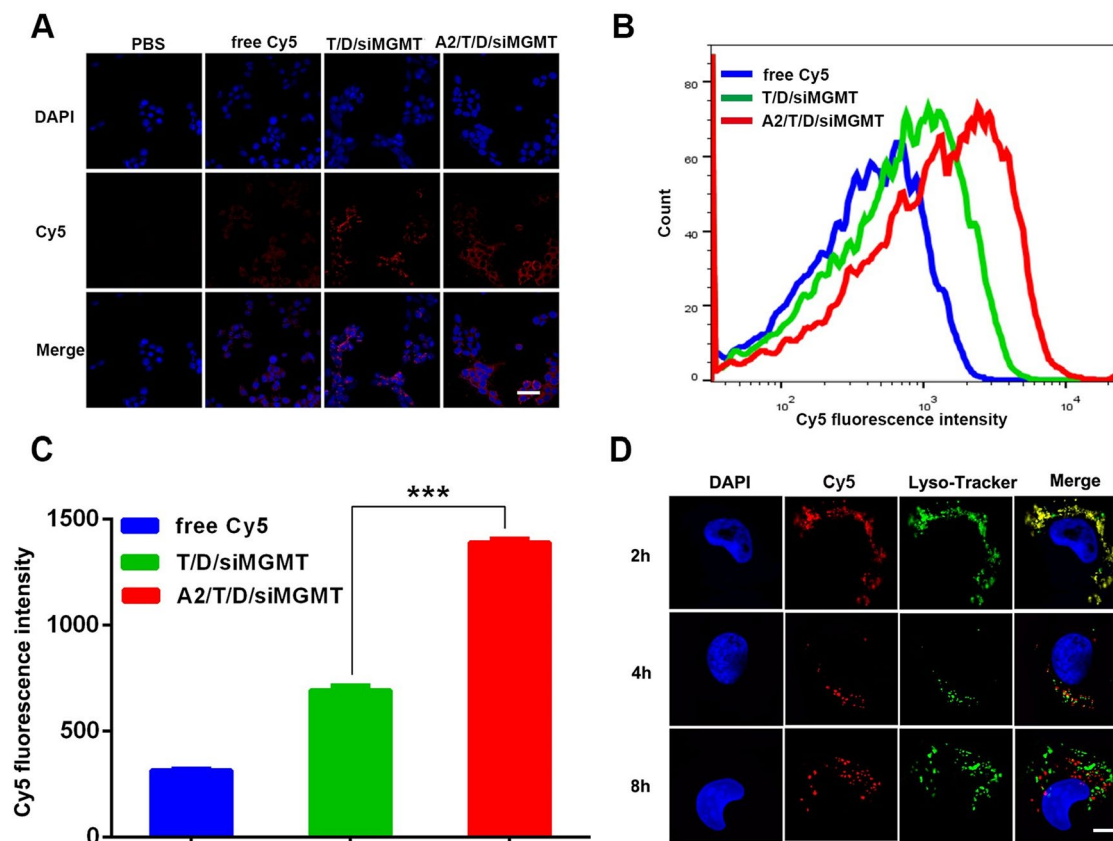


Figure 2. Cellular uptake and endosomal escape of A2/T/D/Cy5-siRNA in T98G cells. (A) CLSM analysis of T98G cells incubated with PBS, free Cy5-siRNA, T/D/Cy5-siRNA and A2/T/D/Cy5-siRNA for 4h (scale bar = 40 μ m). (B) Cellular uptake of free Cy5-siRNA, T/D/Cy5-siRNA and A2/T/D/Cy5-siRNA was analyzed using flow cytometry after 4h incubation and (C) statistical graph. (D) Endosomal escape of A2/T/D/Cy5-siRNA in T98G cells. The nucleus was stained by DAPI, endosome/lysosome was stained by LysoTracker Green, and Cy5-siRNA emitted red fluorescence by itself (scale bar = 10 μ m).

Furthermore, to evaluate whether A2/T/D/Cy5-siRNA can escape from the lysosome of glioma cell, CLSM was used. After T98G cells were incubated with A2/T/D/Cy5-siRNA for 2h, 4h and 8h, intracellular escape was monitored. As shown in Figure 2(D), at 2 hours, red Cy5-siRNA overlapped with green lysosomes, indicating that A2/T/D/Cy5-siRNA was ingested by lysosomes. However, at 4h and 8h, the red Cy5-siRNA deviated from the green lysosome, indicating that the A2/T/D/Cy5-siRNA had escaped from the lysosome. Thus, this delivery system successfully avoided internal lysosomal compartmentalization and released siRNA into the cytoplasm (Xia et al., 2021; Du Rietz et al., 2020).

In vitro cell viability assay

It has been reported that glioma cell lines with high expression of MGMT protein are resistant to TMZ (Chen et al., 2018; Adair et al., 2014; Yi et al., 2019). Therefore, the protein levels of MGMT in different glioma cell lines were evaluated by WB (Figure 3(A)). The MGMT protein level in T98G (1.4) was significantly higher than that in U87 (0.22), LN-229 (0.24) and U251 cells (0.32). Therefore, T98G and U87 cells were used to verify the effect of TMZ. The survival rates of T98G and U87 cells were evaluated by CCK8 experiment. The results showed that the half-maximal inhibitory concentration (IC_{50}) of U87 and T98 were 204.2 ± 0.9 and $491.3 \pm 1.12 \mu$ M respectively (Figure 3(B)). This result showed that T98G cell line was

resistant to TMZ. Subsequently, U87 cells and T98G cells were treated with A2/T/D/CsiRNA and A2/T/D/siMGMT. As show in Figure 3(C), the IC_{50} of U87 cells applied with A2/T/D/CsiRNA and A2/T/D/siMGMT were 180.01 ± 0.69 and 178 ± 1.05 , respectively. However, the IC_{50} of T98G cells incubated with A2/T/D/CsiRNA and A2/T/D/siMGMT were 445.79 ± 0.69 and 241.1 ± 0.84 , respectively (Figure 3(D)). This result indicated that the T98G cell line was no longer resistant to TMZ. As shown in Figure S7, the nanoparticle has little cytotoxicity on normal astrocytes (HA1800). This may be caused by TMZ cannot be released in normal cells.

We further sought to use T98G cells and U87 cells to determine whether the different treatment groups affect cell proliferation. For this, PBS, free TMZ, A2/T/D/CsiRNA and A2/T/D/siMGMT were added to the cells and incubated for 48 hours. EdU results showed that the proliferation rate of other groups was significantly reduced compared with the PBS group in U87 cells. The proliferation rate of T98G cells was slightly decreased in free TMZ and A2/T/D/CsiRNA groups. However, the proliferation rate of T98G cells treated with A2/T/D/siMGMT was significantly decreased (Figure 3(E) and (F)). This indicated that down-regulation of MGMT by iRNA technology can effectively reverse the resistance of T98G to TMZ and reduce cell proliferation.

Calcein-AM (AM) and propidium iodide (PI) solutions, which stain live and dead cells respectively (Wang et al., 2021). Thus, the live/dead assay was used to evaluate the

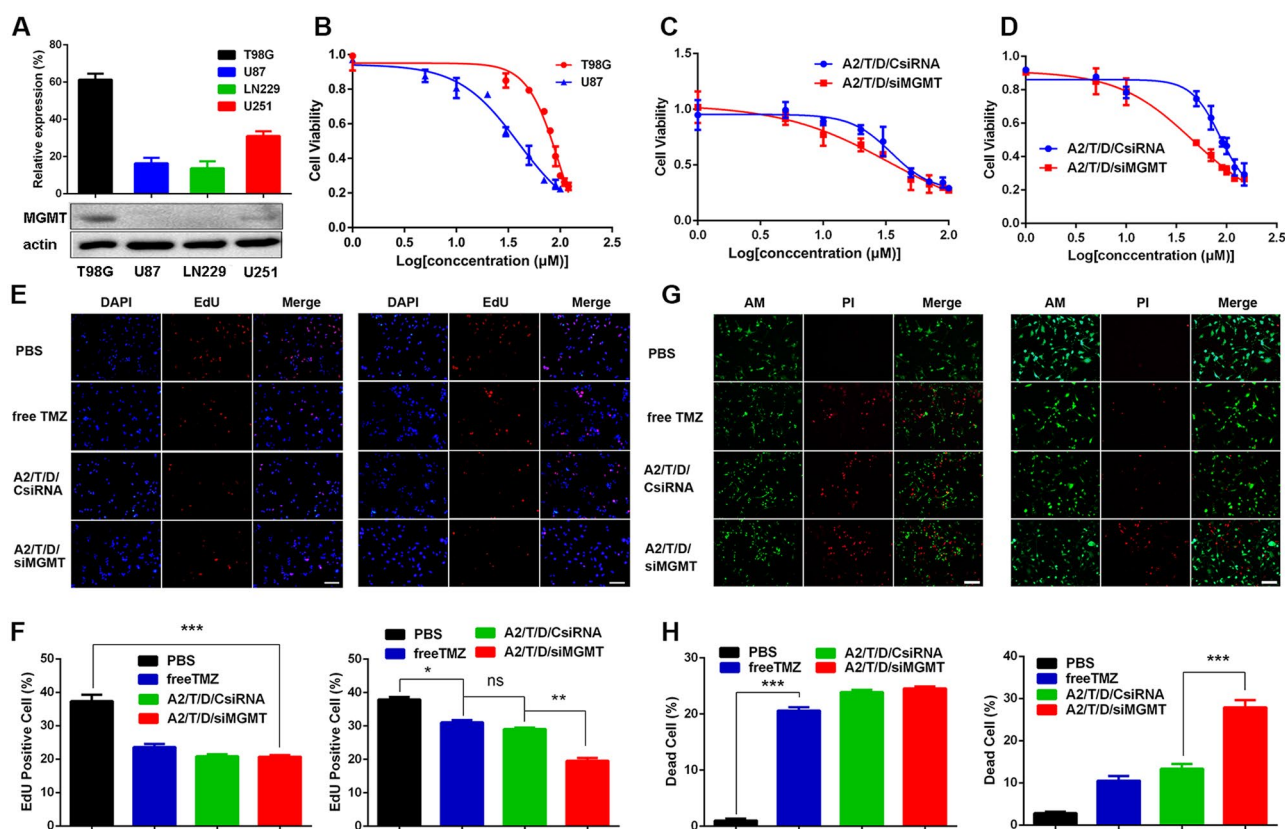


Figure 3. (A) The expression of MGMT protein in T98G, U87, LN-229 and U251 cells by Western blot analysis. (B) A CCK-8 assay was performed to evaluate cell viability in T98G and U87 cells treated with different concentrations of TMZ for 48 h, and CCK8 assay of U87 (C) and T98G (D) treated with A2/T/D/CsiRNA and A2/T/D/siMGMT. (E) EdU proliferation of U87 (left) and T98G (right) cells treated with PBS, free TMZ, A2/T/D/CsiRNA and A2/T/D/siMGMT for 48 h (scale bar = 100 μm). The cells were stained with Apollo 643 (red, representative of EdU) and nuclear specific dye DAPI (blue). (F) Cell number and EdU content of U87 (left) and T98G (right) cells treated with PBS, free TMZ, A2/T/D/CsiRNA and A2/T/D/siMGMT for 48 h. (G) Live/Dead assay on U87 (left) and T98G (right) cells were performed after 48 hours of PBS, free TMZ, A2/T/D/CsiRNA and A2/T/D/siMGMT treatment (scale bar = 100 μm). The live cells were stained with AM (green) and the dead cells were stained with PI (red). (H) Percentage of dead cells of U87 (left) and T98G (right) cells treated with PBS, free TMZ, A2/T/D/CsiRNA and A2/T/D/siMGMT (scale bar = 100 μm). All data are expressed as the means ± SD of values from triplicate experiments (ns $P > 0.05$, * $P < 0.05$, ** $P < 0.01$ and *** $P < 0.001$).

cytotoxicity of nanomedicines on T98G cells and U87 cells. Figure 4(G) and (H) indicated that more than 20% of dead cells were observed in free TMZ, A2/T/D/CsiRNA and A2/T/D/siMGMT treatment groups in the U87 cells. Notably, the number of dead cells using A2/T/D/siMGMT reached 27.9% in T98G. However, only 10.5% and 13.3% dead cells were observed in free TMZ, A2/T/D/CsiRNA treatment groups (Figure 4(G) and (H)). This illustrated that the resistance of T98G to TMZ was successfully reversed.

Construction of U87^{MGMT} and antitumor experiment in vitro

In order to further verify the effect of MGMT expression on the sensitivity of glioma cells to TMZ. The U87^{MGMT} cell line that can stably express MGMT was constructed. Western blot (Figure 4(A)) and qRT-PCR analysis verified the efficiency of upregulation. As shown in Figure 4(B) and (C), MGMT protein and mRNA levels of U87 were up-regulated. This indicated that the U87^{MGMT} cell line with high expression of MGMT was successfully constructed.

Cell viability experiments were further validated on U87^{MGMT}. EdU assay was again performed on U87^{MGMT} cells.

The results that the proliferation rate of U87^{MGMT} cells treated with A2/T/D/siMGMT was significantly decreased (Figure 4(D) and (E)). The live/dead assay indicated that the proportion of dead cell was 24.1% in U87^{MGMT} added with A2/T/D/CsiRNA in Figure 4(F) and (G). As shown in Figure 4(H), the IC_{50} of U87 MGMT incubated with A2/T/D/siMGMT was $213.6 \pm 1.12 \mu\text{M}$. However, the IC_{50} of U87^{MGMT} cells treated with free TMZ and A2/T/D/CsiRNA were $363.4 \pm 0.99 \mu\text{M}$ and $353.03 \pm 1.1 \mu\text{M}$, respectively (Figure 4(H)). The above results indicated that the up-regulation of MGMT led to the drug resistance of U87 cells, and the treatment of A2/T/D/siMGMT successfully enhanced the sensitivity of U87^{MGMT} to TMZ.

Cell apoptosis

We further evaluated the effect of different treatment groups on apoptosis of U87^{MGMT} cells and T98G cells by flow cytometry. As shown in Figure 5(A), in T98G cells and U87^{MGMT} cells, the apoptosis rate of the control group without treatment was account for very small proportion, and the apoptosis rate of cells treated with free TMZ and A2/T/D/CsiRNA was about 5%. In contrast, the apoptosis rate of T98G cells was 14.94%, and the apoptosis rate of U87^{MGMT} cells was as high

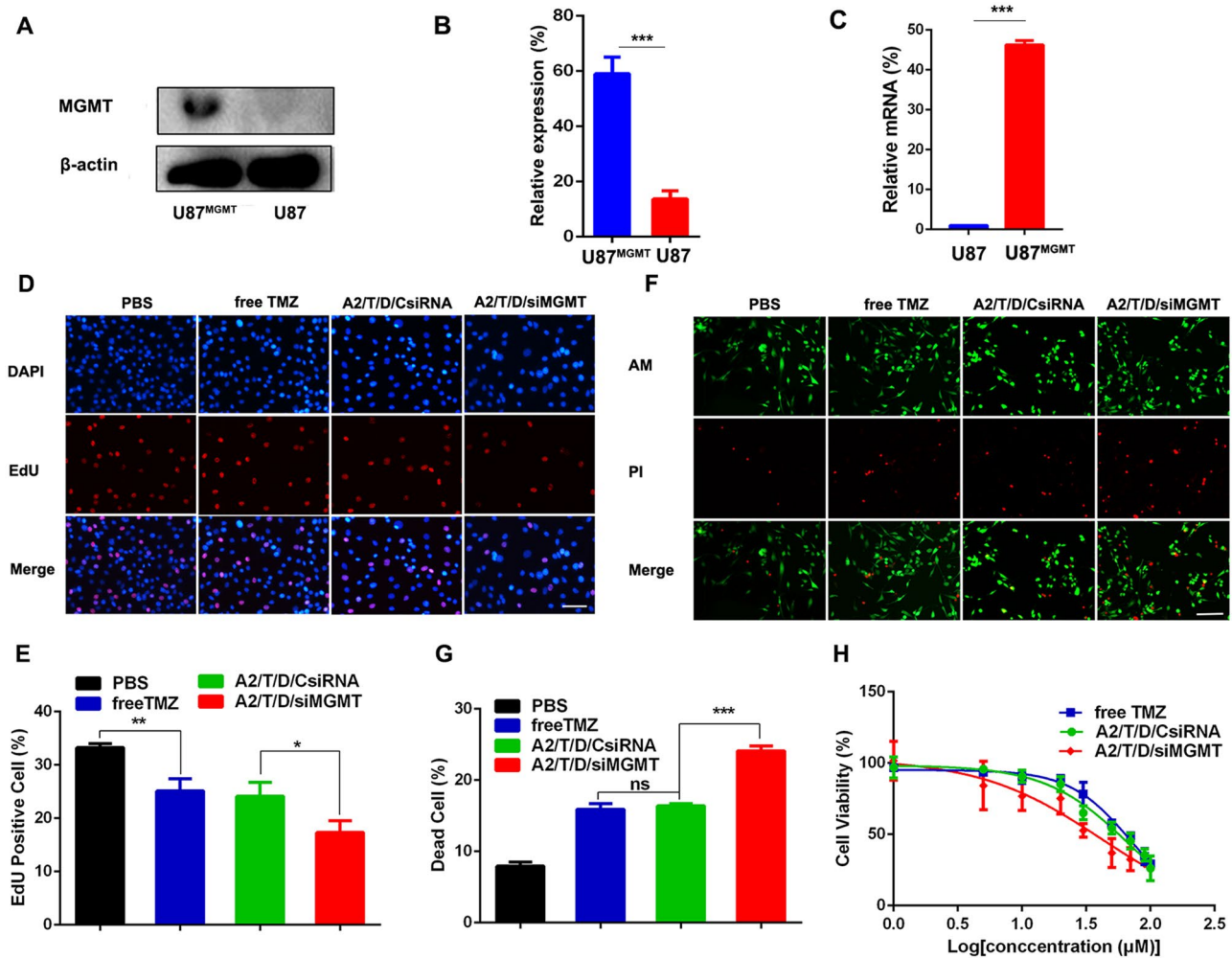


Figure 4. Construction of U87^{MGMT} cell line. The expression of MGMT protein in U87 and U87^{MGMT} (A) and Western blot analysis (B). (C) The relative expression of MGMT mRNA in U87 and U87^{MGMT}. (D) EdU proliferation of U87^{MGMT} cells treated with PBS, free TMZ, A2/T/D/CsiRNA and A2/T/D/siMGMT for 48 h (scale bar = 100 μm). The cells were stained with Apollo 643 (red, representative of EdU) and nuclear specific dye DAPI (blue). (E) Cell number and EdU content of U87^{MGMT} cells treated with PBS, free TMZ, A2/T/D/CsiRNA and A2/T/D/siMGMT for 48 h. (F) Live/Dead assay on U87^{MGMT} cells was performed after 48 hours of PBS, free TMZ, A2/T/D/CsiRNA and A2/T/D/siMGMT treatment (scale bar = 100 μm). The live cells were stained with AM (green) and the live cells were stained with PI (red). Data are shown as mean ± SD ($n=3$), nsP > 0.05, *P < 0.05, **P < 0.01, ***P < 0.001.

as 17.74% in the A2/T/D/siMGMT treatment group. These results further demonstrated that the utilize of siMGMT can increase the sensitivity of TMZ-resistant glioma cells to TMZ (Figure 5(A)).

Gene silencing ability of TMZ-resistant cell lines

Glioma cell lines with high MGMT levels have been recognized as resistant to TMZ. To verify the effects of different treatment groups on the transcription and translation of MGMT, qRT-PCR and Western blotting were exerted respectively. As shown in Figure 5(B) and (C), compared with the control group, the A2/T/D/siMGMT group exhibited significantly enhanced silencing of MGMT protein expression in T98G cells (67.5%) and U87^{MGMT} cells (83%). Meanwhile, qRT-PCR showed that treatment with A2/T/D/siMGMT significantly silenced MGMT gene expression in T98G cells and U87^{MGMT} cells, resulting in 78.8% and 79.1% knockdown of

MGMT mRNA, respectively (Figure 5(D) and (E)). These results were consistent with western blot experiments, and both suggested that A2/T/D/siMGMT performs the strong gene silencing ability of MGMT.

Tumor therapy monitoring in mice

In order to verify the efficacy of NPs in the treatment of glioma in vivo, an orthotopic mouse glioma model of TMZ-resistant U87^{MGMT-Luci} was constructed (Figure 6(A)). Due to the existence of the BBB, it is difficult for general drugs to reach the glioma site (Hua et al., 2021). Therefore, A2 was modified on nanoparticles, and it is expected that A2/T/D/siMGMT can enter glioma site through active targeting (Danhier et al., 2015; Liu et al., 2021). To assess the ability of A2/T/D/siMGMT to cross the BBB and enter glioma tissue, fluorescence imaging was used. First, tumor-bearing nude mice were injected with free Cy5-siRNA, T/D/Cy5-siRNA and

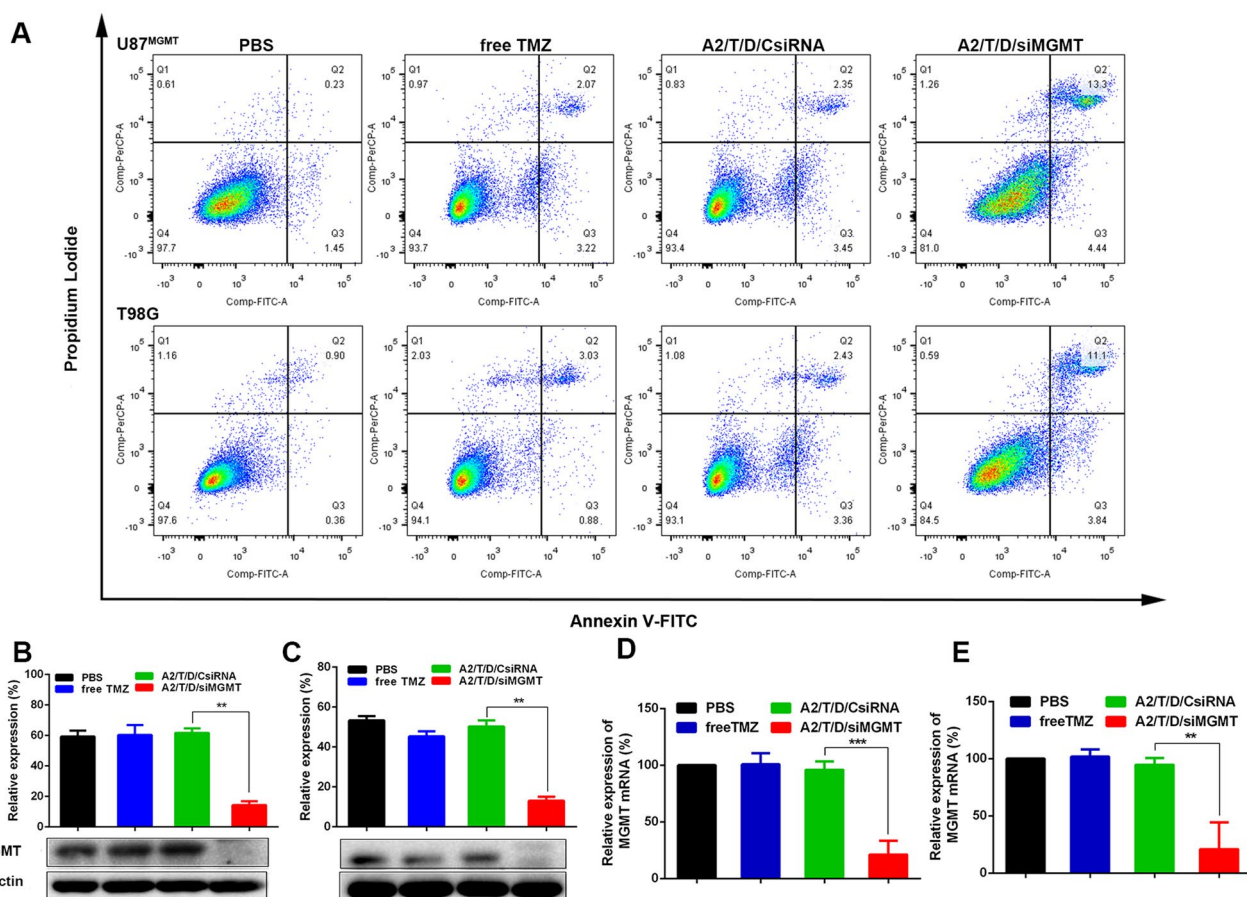


Figure 5. (A) Apoptosis assay was performed in U87^{MGMT} and T98G with flow cytometry using Annexin V-FITC/PI double-staining assay at 24 h after different treatments. Western blot assays were performed to analyze the protein expression levels of MGMT in T98G (B) and U87^{MGMT} (C) cells after treated for 48 h. The silence efficiency of siRNA targeting to MGMT was analyzed by qRT-PCR after treated for 48 h in either T98G (D) or U87^{MGMT} (E) cells. The dose of siMGMT was 1 $\mu\text{g mL}^{-1}$. Data are shown as mean \pm SD ($n=3$), ** $P < 0.01$, *** $P < 0.001$.

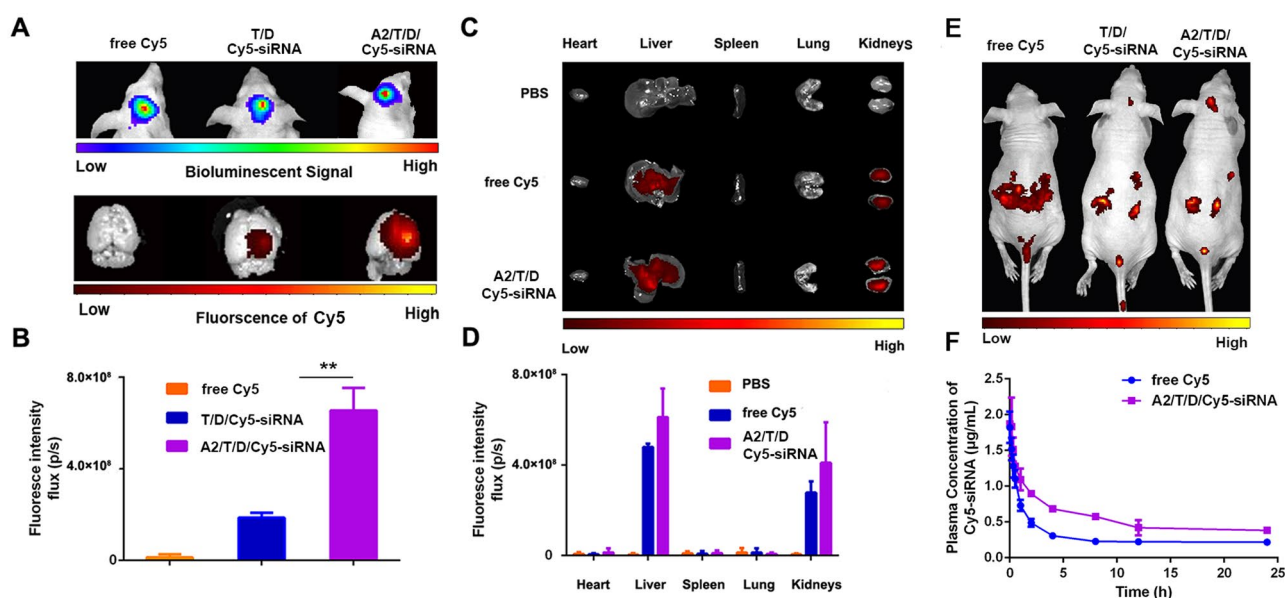


Figure 6. Distribution of Cy5 fluorescence in U87^{MGMT-Luci} tumor-bearing mice. (A) Bioluminescence of luciferase in tumor bearing mice 5 minutes after injection of luciferin potassium solution and Cy5 fluorescence images of excised mouse brains. (B) Quantitative analysis of Cy5 in mouse brain. (C) Tissue biodistribution of PBS, free Cy5-siRNA and A2/T/D/Cy5-siRNA in U87^{MGMT-Luci} tumor-bearing mice after tail vein injection. (D) Quantitative analysis of Cy5 in mouse tissues. (E) In vivo imaging of Cy5 to detect the systemic distribution and targeting ability of A2/T/D/Cy5-siRNA. (F) Blood retention kinetics of free Cy5-siRNA and A2/T/D/Cy5-siRNA (Cy5-siRNA concentration of 1 $\text{mg}\cdot\text{kg}^{-1}$). Data are shown as mean \pm SD ($n=3$).

A2/T/D/Cy5-siRNA via tail vein, respectively. After 4 hours, fluorescence imaging showed the strongest Cy5 fluorescence was observed in the gliomas of mice which injected with A2/T/D/Cy5-siRNA (Figure 6(A), (B) and (E)). The results illustrated that the modification of A2 improved the ability of T/D/Cy5-siRNA to cross BBB and target glioma.

Furthermore, as shown in Figures 6(C) and (E), free Cy5-siRNA and A2/T/D/Cy5-siRNA were rapidly and widely distributed in liver and kidney tissues within 4 h. However, the fluorescence intensity of liver and kidney of mice treated with free Cy5 siRNA was significantly lower than that of mice treated with A2/T/D/Cy5-siRNA. These results indicated that A2/T/D/Cy5-siRNA has a longer serum retention time. Next, the half-life ($t_{1/2}$) of A2/T/D/Cy5-siRNA was measured. As shown in Figure 6(F), free Cy5-siRNA was rapidly eliminated from the blood, with a half-life ($t_{1/2}$) of approximately 0.66 h. In contrast, the half-lives ($t_{1/2}$) of A2/T/D/Cy5-siRNA was approximately 3.86 h. The half-lives ($t_{1/2}$) of A2/T/D/siMGMT and free TMZ were tested with ultraviolet spectrophotometer (Mapata, Shanghai) *in vitro*. As shown in Figure S8, Half-lives

of A2/T/D/siMGMT and free TMZ are 3.65 h and 0.84 h respectively. These increased circulation time would provide a greater chance for A2/T/D/Cy5-siRNA to accumulate in gliomas.

Finally, to verify whether NPs can enhance the sensitivity of TMZ-resistant gliomas to TMZ *in vivo*. A glioma model using U87MGMT-Luci cells was constructed. Mice were divided into 4 groups ($n=7$) according to the fluorescence intensity at day 7 and treated 4 times with PBS, free TMZ, A2/T/D/CsiRNA and A2/T/D/siMGMT, respectively. The bioluminescence intensity of gliomas was measured by fluorescence imaging system every ten days. As shown in Figure 7(A), the tumors of mice treated with PBS progressed rapidly. Based on the drug-resistance of implanted glioma cells to TMZ, mice treated with free TMZ and A2/T/D/CsiRNA also showed higher biofluorescence intensity. However, mice treated with A2/T/D/siMGMT exhibited lower bioluminescence compared to other groups. The results of biological fluorescence statistics showed that the fluorescence intensity of mice treated with PBS on day 27 was 261-fold higher than that on day

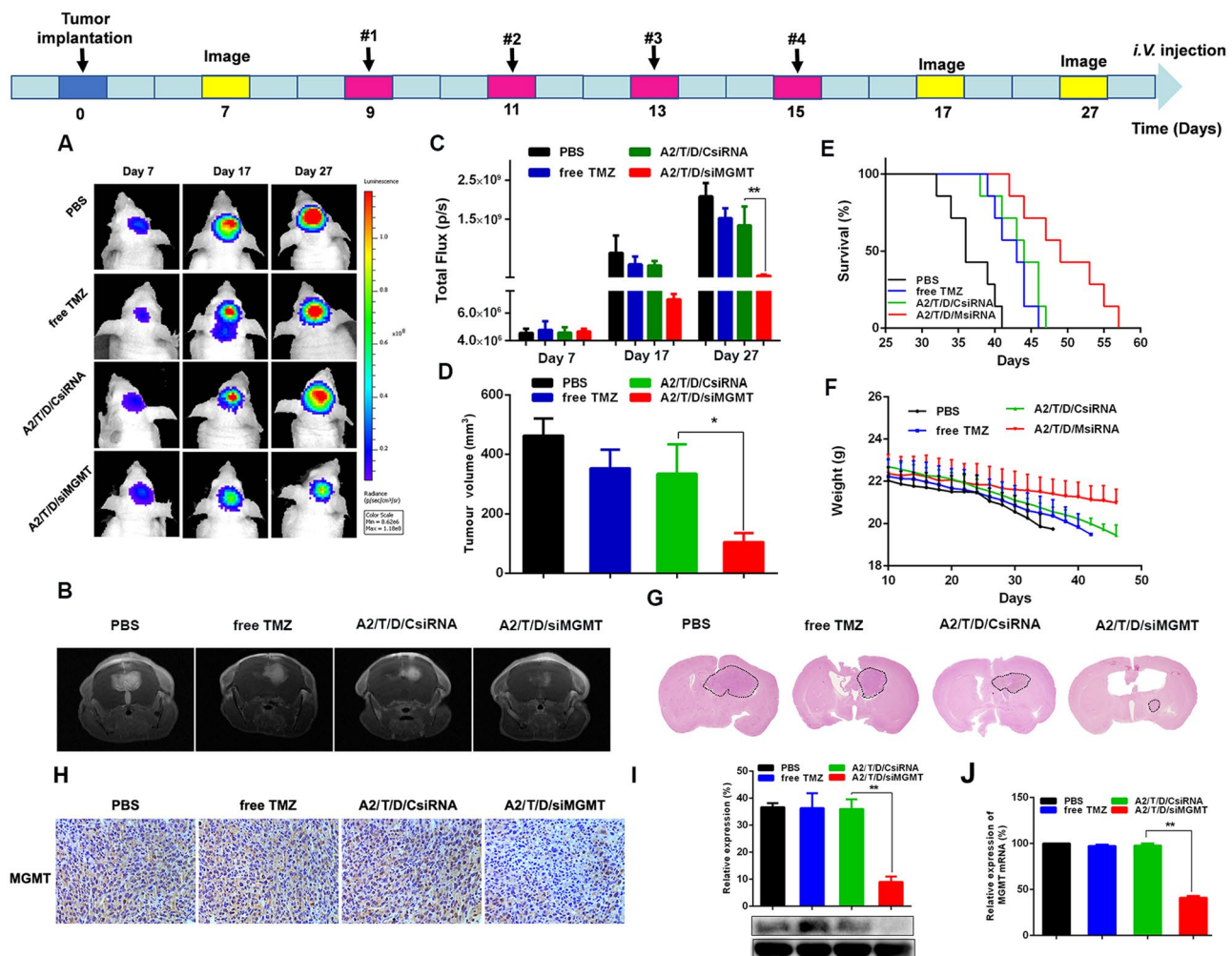


Figure 7. In vivo antitumor efficacy in a TMZ-resistant mouse model. (A) Biofluorescence imaging of U87^{MGMT-Luci} glioma mice with different treatments. (B) T1W images of U87^{MGMT-Luci} glioma mice with different treatments at day 30. (C) Quantification of glioma bioluminescence signal in different treatment groups ($n=3$, $**p < 0.01$). (D) Quantification of glioma volume in different treatment groups ($n=3$, $*p < 0.05$). (E) Kaplan-Meier survival curves of glioma mice in different treatment groups ($n=7$). (F) Body weight monitoring of tumor bearing mice (mean \pm SD, $n=7$). (G) Representative images of H&E-staining of brains sections with orthotopic tumors. (H) Immunohistochemistry staining of MGMT. (I) The expression of MGMT protein in brain tissue by Western blot analysis. (J) (C) The relative expression of MGMT mRNA in brain tissue.

7. The tumor growth rate of mice treated with free TMZ and A2/T/D/CsiRNA was 149-fold and 145-fold higher than at day 7, respectively. However, bioluminescence measurements of mice treated with A2/T/D/siMGMT increased only 34-fold within 27 days (Figure 7(C)). In addition, the fluorescence value of A2/T/D/siMGMT groups was 4.5-fold lower than that of free TMZ treatment on day 27.

In order to intuitively reflect the size of the glioma volume, MRI was applied to mice in different treatment groups on day 30 (Figure 7(B)). The statistical results showed that on the 30th day, the tumor volume of mice treated with PBS, free TMZ and A2/T/D/CsiRNA was 4.42-fold, 3.38-fold and 3.2-fold that of mice treated with A2/T/D/siMGMT (Figure 7(D)). In addition, the results of H&E staining of brain tumor sections were also highly consistent with MRI (Figure 7(G)). These indicated that A2/T/D/siMGMT has high antitumor activity. The combined delivery of siMGMT and P(TMZ)n can effectively reverse the resistance of gliomas with high MGMT expression to TMZ.

Median survival time can objectively reflect the efficacy of drugs. In order to further evaluate the antitumor effect of nanoparticles, the survival time and body weight of tumor-bearing mice were recorded. As shown in Figure 7(E), the median survival time of mice treated with PBS, free TMZ,

A2/T/D/CsiRNA and A2/T/D/siMGMT was 36, 43, 44 and 49, respectively. The survival time of mice treated with A2/T/D/siMGMT was significantly prolonged, and the weight loss was also slower (Figure 7(F)). Ki67 staining, indicating cell proliferation, showed significantly fewer positive nucleus in tumor sections of A2/T/D/siMGMT groups (Figure 8A, C). In addition, apoptotic tumor cells were detected by TUNEL staining of the tumor sections. As shown in Figure 8(B) and (D), A2/T/D/siMGMT caused obvious cell apoptosis. These results suggested that A2/T/D/siMGMT can enhance the sensitivity of glioma to TMZ.

As shown in Figure 6(C), nanoparticles were mainly accumulated in the liver and kidney. Thus, the toxicity of nanoparticles was evaluated by their effects on liver and kidney function, as well as histological changes in major organs. Alanine aminotransferase (ALT) and aspartate aminotransferase (AST) are important indicators of liver dysfunction and exist in the cytoplasm of hepatocytes (Geisinger-Regeneron DiscovEHR Collaboration, 2021). When hepatocyte necrosis, ALT and AST may rise rapidly and be measured sensitively. The nanoparticles showed limited influence, hardly exhibited obvious hepatic cytolysis (Figure 8(F) and (G)). Furthermore, blood urea nitrogen (BUN) and creatinine (CREA) were used to evaluate the kidney function. As show in Figure 8(H) and

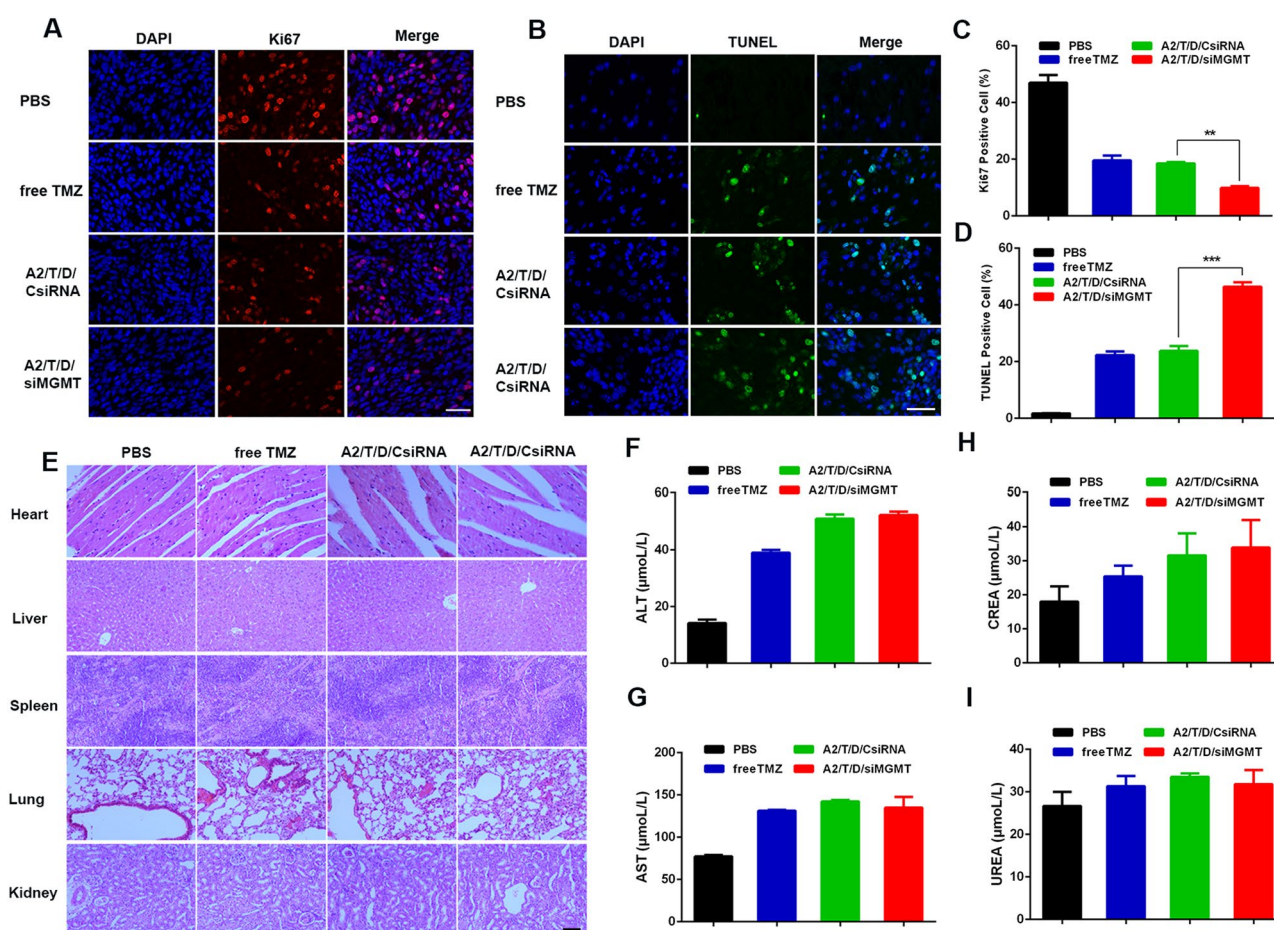


Figure 8. Antitumor effect and safety evaluation in different treatment groups. Therapeutic effect on proliferation by Ki67 (A) and apoptosis by TUNEL (scale bar = 100 μm). (B) staining of the dissected tumor tissue (scale bar = 100 μm). Graphical illustrated the quantification of Ki-67 (C) and TUNEL (D) positive cells percentage. (E) Representative H&E staining of major organs (heart, liver, spleen, lung and kidney) (scale bar = 200 μm). Plasma biochemistry analyses revealing the levels of ALT (F), AST (G), CREA (H), and BUN (I) in mice treated with PBS, free TMZ, A2/T/D/CsiRNA and A2/T/D/siMGMT. The results are present as mean \pm SD ($n=3$).

(I), the function indices of BUN and CREA were within the normal range. These suggested that the nanoparticles do not have significant renal damage. Finally, the H&E staining images of the major organs (heart, liver, spleen, lung and kidney) indicated that no noticeable tissue damage in morphology (Figure 8(E)). These indicated that the nanoparticles can not only effectively reverse the resistance of gliomas with high expression of MGMT to TMZ, but also have good biosafety.

Discussion

TMZ is a conventional chemotherapeutic drug for glioma, however, its clinical application and efficacy is severely restricted by its drug resistance properties⁴¹. O6-methylguanine-DNA methyltransferase is a DNA repair enzyme, which can repair the DNA damage caused by TMZ. A large number of clinical data show that reducing the expression of MGMT can enhance the chemotherapeutic efficacy of TMZ³³. Therefore, in order to improve the resistance of glioma to TMZ, an A2 modified nanoprodru of P(TMZ)_n that combines with siMGMT targeting MGMT was developed (A2/T/D/siMGMT).

In this study, the cationic polymer DOTAP was used to deliver MGMT siRNA to reverse the resistance of glioma cells to TMZ. The average particle size and zeta potential of A2/T/D/siMGMT were 61.71 nm and 3.74 MV, respectively. These results illustrate that it is possible for nanoparticles to penetrate the BBB. In addition, A2 was modified on nano-carriers to make it easier for nanoparticles were taken up by glioma cells. A2 modified nanocomplexes show better delivery efficiency than nontargeted ones. CLSM results also showed that A2/T/D/siMGMT successfully escaped from the lysosome of glioma cells, after 4 hours of NPs were treated, which would lead to the increased gene silencing activity of MGMT.

As we all know, the key of siRNA therapy is the ability of gene silencing. qRT-PCR and WB results showed that A2/T/D/siMGMT could significantly inhibit the expression of MGMT gene. In addition, the expression level of MGMT protein in U87^{MGMT} cells suggested that the TMZ resistant cell line U87^{MGMT} was successfully constructed. CCK8 and apoptosis detection also indicated that the combined application of P (TMZ) _n and MGMT siRNA had a notable effect on apoptosis by reducing the expression of MGMT and improved the anti-cancer effect in vitro.

In order to study the targeting ability of nanoparticles, U87^{MGMT} cell glioma model was constructed. Cy5 was injected into U87^{MGMT-Lucif} tumor bearing mice through caudal vein. The results showed that A2/T/D/Cy5-siMGMT could penetrate the BBB and accumulate mainly in the liver and kidney.

In vivo studies illustrated that mice treated with A2/T/D/siMGMT had significantly longer survival time and the slowest weight loss. Studies have shown that the combination of P (TMZ) _n and MGMT siRNA can effectively enhance the high sensitivity of temozolomide and significantly inhibit the growth of glioma. In addition, mice treated with A2/T/D/

siMGMT had no obvious toxic and side effects. Therefore, A2/T/D/siMGMT has the potential to treat glioma.

Disclosure statement

The authors declare no conflict of interest arising from this work.

Funding

This work was supported by a grant from the National Natural Science Foundation of China [no. 82072796]. This work was also financed by the Social Development Project of Jiangsu Department of Science and Technology [BE2020642] and Postgraduate Research & Practice Innovation Program of Jiangsu Province [KYCX21_2657 and KYCX22_2950]. Research was supported by General project of Jiangsu Provincial Health Commission [M2020081].

References

- Adair JE, Johnston SK, Mrugala MM, et al. (2014). Gene therapy enhances chemotherapy tolerance and efficacy in glioblastoma patients. *J Clin Invest* 124:4082–92.
- Basuki JS, Duong HT, Macmillan A, et al. (2013). Using fluorescence lifetime imaging microscopy to monitor theranostic nanoparticle uptake and intracellular doxorubicin release. *ACS Nano* 7:10175–89.
- Chen X, Zhang M, Gan H, et al. (2018). A novel enhancer regulates MGMT expression and promotes temozolomide resistance in glioblastoma. *Nat Commun* 9:2949.
- Danhier F, Messaoudi K, Lemaire L, et al. (2015). Combined anti-galectin-1 and anti-EGFR siRNA-loaded chitosan-lipid nanocapsules decrease temozolomide resistance in glioblastoma: in vivo evaluation. *Int J Pharm* 481:154–61.
- Du K, Xia Q, Heng H, Feng F. (2020). Temozolomide-doxorubicin conjugate as a double intercalating agent and delivery by apoferritin for glioblastoma chemotherapy. *ACS Appl Mater Interfaces* 12:34599–609.
- Du Rietz H, Hedlund H, Wilhelmson S, et al. (2020). Imaging small molecule-induced endosomal escape of siRNA. *Nat Commun* 11:1809.
- Hanafy AS, Dietrich D, Fricker G, Lamprecht A. (2021). Blood-brain barrier models: rationale for selection. *Adv Drug Deliv Rev* 176:113859.
- Hua D, Tang L, Wang W, et al. (2021). Improved antiglioblastoma activity and BBB permeability by conjugation of paclitaxel to a cell-penetrative MMP-2-cleavable peptide. *Adv Sci (Weinh)* 8:2001960.
- Hua L, Wang Z, Zhao L, et al. (2018). Hypoxia-responsive lipid-poly(hypoxic radiosensitized polyprodrug) nanoparticles for glioma chemo- and radiotherapy. *Theranostics* 8:5088–105.
- Islam Y, Leach AG, Smith J, et al. (2021). Physiological and pathological factors affecting drug delivery to the brain by nanoparticles. *Adv Sci (Weinh)* 8:e2002085.
- Jiang T, Qiao Y, Ruan W, et al. (2021). Cation-free siRNA micelles as effective drug delivery platform and potent RNAi nanomedicines for glioblastoma therapy. *Adv Mater* 33:e2104779.
- Johnson KC, Anderson KJ, Courtois ET, et al. (2021). Single-cell multi-modal glioma analyses identify epigenetic regulators of cellular plasticity and environmental stress response. *Nat Genet* 53:1456–68.
- Joshi N, Yan J, Levy S, et al. (2018). Towards an arthritis flare-responsive drug delivery system. *Nat Commun* 9:1275.
- Joshi SK, Qian K, Bisson WH, et al. (2020). Discovery and characterization of targetable NTRK point mutations in hematologic neoplasms. *Blood* 135:2159–70.
- Kang S, Duan W, Zhang S, et al. (2020). Muscone/RI7217 co-modified upward messenger DTX liposomes enhanced permeability of blood-brain barrier and targeting glioma. *Theranostics* 10:4308–22.

- Karlsson J, Luly KM, Tzeng SY, Green JJ. (2021). Nanoparticle designs for delivery of nucleic acid therapeutics as brain cancer therapies. *Adv Drug Deliv Rev* 179:113999.
- Kleber S, Sancho-Martinez I, Wiestler B, et al. (2008). Yes and PI3K bind CD95 to signal invasion of glioblastoma. *Cancer Cell* 13:235–48.
- Liu J, Chang J, Jiang Y, et al. (2019). Fast and efficient CRISPR/Cas9 genome editing in vivo enabled by bioreducible lipid and messenger RNA nanoparticles. *Adv Mater* 31:e1902575.
- Liu Y, Zheng M, Jiao M, et al. (2021). Polymeric nanoparticle mediated inhibition of miR-21 with enhanced miR-124 expression for combinatorial glioblastoma therapy. *Biomaterials* 276:121036.
- Meng X, Zhao Y, Han B, et al. (2020). Dual functionalized brain-targeting nanoinhibitors restrain temozolomide-resistant glioma via attenuating EGFR and MET signaling pathways. *Nat Commun* 11:594.
- Nicholson JG, Fine HA. (2021). Diffuse glioma heterogeneity and its therapeutic implications. *Cancer Discov* 11:575–90.
- Otvos B, Alban TJ, Grabowski MM, et al. (2021). Preclinical modeling of surgery and steroid therapy for glioblastoma reveals changes in immunophenotype that are associated with tumor growth and outcome. *Clin Cancer Res* 27:2038–49.
- Qiao C, Yang J, Shen Q, et al. (2018). Traceable nanoparticles with dual targeting and ROS response for RNAi-based immunochemotherapy of intracranial glioblastoma treatment. *Adv Mater* 30:e1705054.
- Setten RL, Rossi JJ, Han SP. (2019). The current state and future directions of RNAi-based therapeutics. *Nat Rev Drug Discov* 18:421–46.
- Sita TL, Kouri FM, Hurley LA, et al. (2017). Dual bioluminescence and near-infrared fluorescence monitoring to evaluate spherical nucleic acid nanoconjugate activity in vivo. *Proc Natl Acad Sci U S A* 114:4129–34.
- Tan AC, Ashley DM, Lopez GY, et al. (2020). Management of glioblastoma: state of the art and future directions. *CA Cancer J Clin* 70:299–312.
- Tan J, Duan X, Zhang F, et al. (2020). Theranostic nanomedicine for synergistic chemodynamic therapy and chemotherapy of orthotopic glioma. *Adv Sci (Weinh)* 7:2003036.
- Tian M, Xing R, Guan J, et al. (2021). A nanoantidote alleviates glioblastoma chemotoxicity without efficacy compromise. *Nano Lett* 21:5158–66.
- Wang K, Kievit FM, Chiarelli PA, et al. (2021). siRNA nanoparticle suppresses drug-resistant gene and prolongs survival in an orthotopic glioblastoma xenograft mouse model. *Adv Funct Mater* 31(6):2007166.
- Wang M, Lv CY, Li SA, et al. (2021). Near infrared light fluorescence imaging-guided biomimetic nanoparticles of extracellular vesicles deliver indocyanine green and paclitaxel for hyperthermia combined with chemotherapy against glioma. *J Nanobiotechnology* 19:210.
- Wang Y, Jiang Y, Wei D, et al. (2021). Nanoparticle-mediated convection-enhanced delivery of a DNA intercalator to gliomas circumvents temozolomide resistance. *Nat Biomed Eng* 5:1048–58.
- Wang Z, Zhang H, Xu S, et al. (2021). The adaptive transition of glioblastoma stem cells and its implications on treatments. *Signal Transduct Target Ther* 6:124.
- Ward LD, Tu HC, Quenneville CB, Geisinger-Regeneron DiscovEHR Collaboration, et al. (2021). GWAS of serum ALT and AST reveals an association of SLC30A10 Thr95Ile with hypermanganesemia symptoms. *Nat Commun* 12:4571.
- Xia Y, Tang G, Chen Y, et al. (2021). Tumor-targeted delivery of siRNA to silence Sox2 gene expression enhances therapeutic response in hepatocellular carcinoma. *Bioact Mater* 6:1330–40.
- Xu H, Han Y, Zhao G, et al. (2020). Hypoxia-responsive lipid-polymer nanoparticle-combined imaging-guided surgery and multitherapy strategies for glioma. *ACS Appl Mater Interfaces* 12:52319–28.
- Xu J, Liu Y, Liu S, et al. (2022). Metformin bicarbonate-mediated efficient RNAi for precise targeting of TP53 deficiency in colon and rectal cancers. *Nano Today* 43:101406.
- Yang K, Wu Z, Zhang H, et al. (2022). Glioma targeted therapy: insight into future of molecular approaches. *Mol Cancer* 21:39.
- Yi GZ, Huang G, Guo M, et al. (2019). Acquired temozolomide resistance in MGMT-deficient glioblastoma cells is associated with regulation of DNA repair by DHC2. *Brain* 142:2352–66.
- Zhang XN, Yang KD, Chen C, et al. (2021). Pericytes augment glioblastoma cell resistance to temozolomide through CCL5-CCR5 paracrine signaling. *Cell Res* 31:1072–87.
- Zoulikha M, Xiao Q, Bofo GF, et al. (2022). Pulmonary delivery of siRNA against acute lung injury/acute respiratory distress syndrome. *Acta Pharm Sin B* 12:600–20.